

Ultrasonic welding of polymer optical fibres onto composite materials

S. Shimada, H. Tanaka, K. Hasebe, N. Hayashi, Y. Ochi, T. Matsui, I. Nishizaki, Y. Matsumoto, Y. Tanaka, H. Nakamura, Y. Mizuno[✉] and K. Nakamura

The ultrasonic welding of polymer optical fibres (POFs) onto carbon-fibre-reinforced polymers for advanced fibre-optic sensing is demonstrated. The relationships among the welding time, preload, optical loss, and adhesive force are fully evaluated. A high-speed camera to monitor changes in the cross section of the POF during the ultrasonic welding is also used.

Introduction: The age-induced degradation and seismic damage of steel structures have recently become a serious social problem. One solution to this problem involves utilising carbon-fibre-reinforced polymers (CFRPs) – composite materials that offer a high strength-to-weight ratio and rigidity – as reinforcing materials [1–4]. CFRPs can be fabricated in various ways. One low-cost fabrication technique is vacuum-assisted resin transfer moulding (VaRTM) [2, 3], wherein the resin is infused into dry fabrics formed on a mould under vacuum pressure. There exists a considerable demand for effective health-monitoring techniques of the CFRP-reinforced components [3, 4].

One of the most promising monitoring techniques is fibre-optic sensing with distributed strain and temperature measurement capability [5]. As the glass optical fibres commonly used in such sensors are relatively easily damaged, an increasing amount of attention has been paid to the use of plastic optical fibres (POFs) [6, 7], which possess much larger core diameters (up to ~1 mm) and extremely high flexibilities. Accordingly, the use of POFs in the field is significantly more practical, as they pose a much lower risk of fibre breakage. Conventionally, adhesive materials (such as epoxy glue) are often used to fix the POFs onto the surface of the CFRPs, but this method poses two problems: (i) the waiting time required for the adhesive to harden is long (several minutes or longer), and (ii) the deformation of the CFRP, which should be detected by the fibre sensor, becomes absorbed by the adhesive layer.

To mitigate these problems, in this study we develop a new technique for fixing the POFs onto the surface of the CFRPs, which is based on ultrasonic welding [8, 9]. In our experiment, the POFs are successfully welded onto the CFRP surfaces within a few seconds. We then measure the optical propagation loss of the POFs as a function of welding time, and investigate the adhesive force as a function of the preload.

Principle and setup: Ultrasonic welding is one of the most popular methods for joining thermoplastics because of its high-speed, low-cost operation and ease of automation [8]. To give a typical example, ultrasonic oscillation at several dozen kilohertz is applied to stacked sheets of thermoplastics under some preload. The boundaries of the plastics then generate frictional heat, leading to melting and welding [8]. This technique is suitable for POFs with relatively low glass-transition temperatures (~100 °C) [6] and is not applicable to glass optical fibres.

In the experiment, we used POF samples with a core diameter of 0.98 mm, a cladding diameter of 1.0 mm, and an optical propagation loss of 0.25 dB/m at a wavelength of 650 nm. The samples were mainly composed of polymethyl methacrylate, which is a thermoplastic material. In contrast, the base material of the CFRP sheet samples (0.85 mm thick and fabricated by VaRTM) was epoxy resin, which is known as a thermoset plastic; thus, the CFRP samples themselves did not melt. However, melted POFs were so firmly welded to the rough surface of the CFRP samples that the POFs precisely followed the deformation (strain and/or bending) of the CFRPs.

During ultrasonic welding of the POF, additional optical loss is inevitably induced according to the change in the cross-sectional shape of the fibre core. Therefore, the transmitted light power was plotted as a function of the welding time (defined as the time after the ultrasonic oscillation was first applied). The experimental setup is depicted in Fig. 1a. A semiconductor laser with a wavelength of 641 nm and an output power of 1.5 mW was used as a light source. We employed a Langevin-type transducer with a cylindrical horn and a flat tip (tip diameter: 30 mm; oscillation frequency: 29 kHz; oscillation amplitude: 31 μm), the position of which was fixed after the initial preload was set to a desired value (verified using a weight scale). A silicone

rubber sheet was placed at the bottom of the CFRP sheet to absorb the ultrasonic oscillations. The transmitted light was guided to a photo detector, and its electrical output was monitored using an oscilloscope; this configuration enabled the transmitted light power measurements to be performed in real-time during the welding process. The change in the cross-sectional shape of the POF during the welding process was simultaneously monitored using a high-speed camera at 1000 fps.

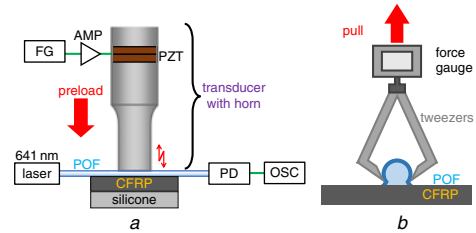


Fig. 1 Schematic setup

a Setup for ultrasonic welding of POFs. AMP: amplifier; CFRP: carbon-fibre-reinforced polymer; FG: function generator; OSC: oscilloscope; PD: photo detector; PZT: lead zirconate titanate
b Setup for measuring the POF-to-CFRP adhesion force

The POF-to-CFRP adhesion force was also evaluated. First, 100 mm long POF samples were welded onto the CFRP sheets under different preloads (welded length: ~30 mm; welding time: 1 s). Then, as shown in Fig. 1b, the welded POFs were nipped with tweezers (tip width: ~5 mm) that were connected to a force gauge, which was gradually lifted upward. In this evaluation, the POF-to-CFRP adhesion force was defined as the force at which the welded bottom of the POF began to peel.

Experimental results: Fig. 2a shows the transmitted light power as a function of the welding time. The initial preloads were varied from 3 to 20 N. The vertical axis was normalised so that the optical power under preload before welding was 1. As the preload increased (resulting in a larger deformation of the POF), the optical power tended to decrease rapidly. To quantitatively evaluate this behaviour, we plotted the preload dependence of the welding time required for the normalised transmitted power to decrease to 0.8 (Fig. 2b). We found that the required welding time exponentially decayed as the preload increased. Note that, in Fig. 2a, the transmitted power ultimately decreased to 0 for all the preloads. By repeated experiments, we found that this was either because the cross-section of the POF was completely crushed (for relatively high preloads) or because the POF was cut (for relatively low preloads). The latter phenomenon can be explained as follows. As the POF melted, a gap was generated between the horn and the POF; then, owing to the deflection of the POF, the ultrasonic oscillation was locally applied to a certain point of the POF. This mechanism can also explain the unstable behaviour that is observed after 5 s of welding for relatively low preloads (see Fig. 2a).

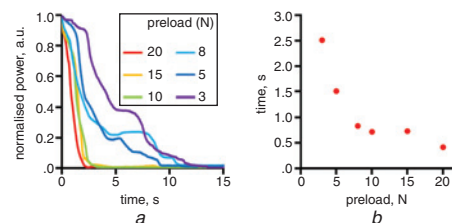


Fig. 2 Measured results

a Normalised transmitted light power as a function of welding time under different initial preloads
b Relationship between the preload and the time required for the normalised power to decrease to 0.8

We then observed the change in the cross section of the POF during the ultrasonic welding using a high-speed camera. The initial preload was set to 8 N. Fig. 3a shows the normalised transmitted light power as a function of the welding time t ; the photographs taken at the corresponding welding times ($t = 0, 0.3, 0.6,$ and 1.0 s) are shown in Figs. 3b–e, respectively. Only the portions of the POF that touched the CFRP surface were observed to melt. This is because the friction coefficient

at the boundary between the POF and the rough surface of the CFRP was larger than that at the boundary between the POF and the smooth surface of the transducer horn. This behaviour is preferable to the undesired increase in optical loss.

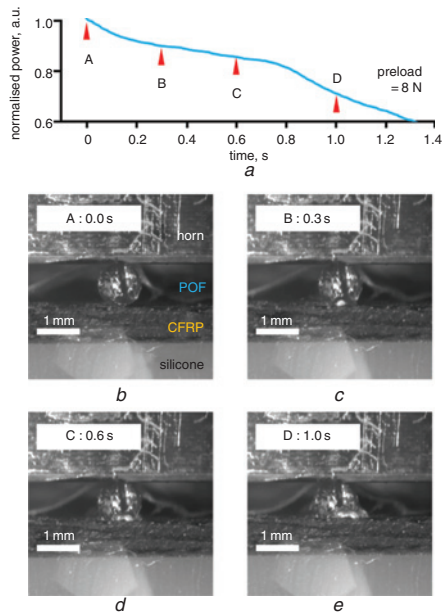


Fig. 3 High-speed monitoring results
a Normalised transmitted light power as a function of welding time under an 8 N preload (magnified view of Fig. 2*a*)
b–e High-speed micrographs of the ultrasonically welded POF at 0.0, 0.3, 0.6, and 1.0 s, respectively

Finally, the adhesive force of the welded POF was measured with respect to the preload (Fig. 4). For each preload, the same measurement was performed 5 times, and the average values were plotted with error bars that represent their standard deviations. For low preloads of <5 N, the POF was not welded onto the CFRP surface. As the preload increased, the adhesive force increased; this behaviour is valid, considering that the higher preload induces larger deformation of the POF (at $t = 1$ s in this measurement), leading to a larger melted area and a more complete adhesion onto the rough surface of the CFRP. Thus, a trade-off relationship between the optical loss and the adhesive force was experimentally verified. Note that the adhesive force can be significantly augmented by welding multiple points of a single POF. The continuous welding of a single POF in the longitudinal direction could thus lead to a high adhesive force.

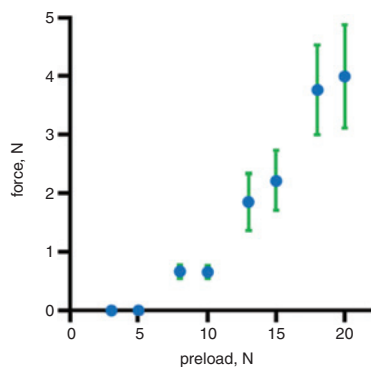


Fig. 4 Adhesive force as a function of the preload (welding time $t = 1$ s)

Conclusion: By exploiting the ultrasonic welding technique, we demonstrated a new procedure for rapidly fixing POFs onto CFRP surfaces. The time required for the POF welding was on the order of seconds, which was far shorter the time associated with conventional methods. The optical propagation loss of the POFs and the

POF-to-CFRP adhesive force were then quantitatively evaluated, and we found that there exists a trade-off relationship between these two quantities. The adhesive force can be drastically enhanced either by the multipoint/continuous welding of the POF or by the use of special CFRPs, the base materials of which are comprised of thermoplastics. We anticipate that this technique can also be used to fix and embed the POFs in the CFRPs, especially during the VaRTM process, and that these results will be useful in applying POF-based sensing technology to the health monitoring of composite materials.

Acknowledgments: This work was supported by MLIT Construction Technology Research and Development Subsidy Program and by JSPS KAKENHI Grant Numbers 25709032, 26630180, and 25007652.

© The Institution of Engineering and Technology 2016

Submitted: 18 March 2016 E-first: 22 July 2016

doi: 10.1049/el.2016.0905

One or more of the Figures in this Letter are available in colour online.

S. Shimada, H. Tanaka, K. Hasebe, Y. Mizuno and K. Nakamura (Laboratory for Future Interdisciplinary Research of Science and Technology, Tokyo Institute of Technology, Yokohama 226-8503, Japan)

✉ E-mail: ymizuno@sonic.pi.titech.ac.jp

N. Hayashi (Research Center for Advanced Science and Technology, The University of Tokyo, Tokyo 153-8904, Japan)

Y. Ochi (Advanced Composites Center, Toray Industries, Inc., Nagoya 455-0024, Japan)

T. Matsui (First Advanced Composites Technical Department, Toray Industries, Inc., Nagoya 455-0024, Japan)

I. Nishizaki (Innovative Materials and Resources Research Center, Public Works Research Institute, Ibaraki 305-8516, Japan)

Y. Matsumoto (Department of Architecture and Civil Engineering, Toyoashi University of Technology, Aichi 441-8580, Japan)

Y. Tanaka (Institute of Engineering, Tokyo University of Agriculture and Technology, Tokyo 184-8588, Japan)

H. Nakamura (Department of Civil and Environmental Engineering, Tokyo Metropolitan University, Tokyo 192-0397, Japan)

References

- Uddin, N.: 'Developments in Fiber-Reinforced Polymer (FRP) composites for civil engineering' (Woodhead Publishing, Oxford, 2013)
- Lin, L.Y., Lee, J.H., Hong, C.E., Yoo, G.H., and Advani, S.G.: 'Preparation and characterization of layered silicate/glass fiber/epoxy hybrid nanocomposites via vacuum-assisted resin transfer molding (VaRTM)', *Compos. Sci. Technol.*, 2006, **66**, (13), pp. 2116–2125, doi: 10.1016/j.compscitech.2005.12.025
- Takeda, N.: 'Characterization of microscopic damage in composite laminates and real-time monitoring by embedded optical fiber sensors', *Int. J. Fatigue*, 2002, **24**, (2–4), pp. 281–289, doi: 10.1016/S0142-1123(01)00083-4
- Hamouda, T., Seyam, A.F.M., and Peters, K.: 'Evaluation of the integrity of 3D orthogonal woven composites with embedded polymer optical fibers', *Compos. B, Eng.*, 2015, **78**, pp. 79–85, doi: 10.1016/j.compositesb.2015.03.092
- Mizuno, Y., Zou, W., He, Z., and Hotate, K.: 'Proposal of Brillouin optical correlation-domain reflectometry (BOCDR)', *Opt. Express*, 2008, **16**, (16), pp. 12148–12153, doi: 10.1364/OE.16.012148
- Kuzyk, M.G.: 'Polymer fiber optics: materials, physics, and applications' (CRC Press, Boca Raton, 2006)
- Hayashi, N., Mizuno, Y., and Nakamura, K.: 'Distributed Brillouin sensing with centimeter-order spatial resolution in polymer optical fibers', *J. Lightw. Technol.*, 2014, **32**, (21), pp. 3397–3401, doi: 10.1109/JLT.2014.2339361
- Benatar, A.: 'Ultrasonic welding of plastics and polymeric composites', in Gallego-Juarez, J.A., and Graff, K.F. (eds.): 'Power ultrasonics: applications of high-intensity ultrasound' (Woodhead Publishing, Cambridge, 2015)
- Mizuno, Y., Ohara, S., Hayashi, N., and Nakamura, K.: 'Ultrasonic splicing of polymer optical fibres', *Electron. Lett.*, 2014, **50**, (19), pp. 1384–1386, doi: 10.1049/el.2014.1224